

# Product angular and alignment distributions in photodissociation from Rydberg states: NO, O<sub>2</sub> and N<sub>2</sub>O

Paul L. Houston

*Baker Laboratory of Chemistry, Cornell University, Ithaca, NY 14853 USA*

## I. TWO-PHOTON EXCITATION AND DISSOCIATION THROUGH NO RYDBERG LEVELS

Despite reports of excitation spectra and product analysis, it is only recently that product imaging has been used to investigate angular distributions of the products of NO predissociation from Rydberg states. We have investigated dissociation of NO Rydberg states using two-photon excitation to populate the  $8d\pi^-(v=1)$ , the  $6d\pi^-(v=1)/5s\sigma(v=3)$ , and the  $5s\sigma(v=2)$  Rydberg levels in jet-cooled NO at wavelengths near 265, 270 and 278 nm, respectively. These states, excited at relatively low powers, show rotational resolution. Velocity mapped images of the dissociation product O(<sup>3</sup>P<sub>2</sub>) were recorded at various rotational lines in these regions, and the resulting angular distributions were compared to quantum mechanical theoretical calculations. Not only do the angular distributions aid in confirming spectral assignments, they also distinguish between  $\Sigma$ ,  $\Pi$ , and  $\Delta$  intermediate states in the two-photon excitation.

Our spectra of jet-cooled NO can be recorded either by monitoring the NO<sup>+</sup> created by a third photon following two-photon excitation of the Rydberg or by monitoring the O atom produced by the dissociation and detected by a second laser tuned to the 2+1 ionization wavelength near 226 nm. In the case of the  $8d\pi^-(v=1)$  level and the  $5s\sigma(v=2)$  level, our spectra are very similar to those obtained earlier by Pratt *et al.* [1] The most interesting spectrum is one we assign to an overlap between the  $6d\pi^-(v=1)$  and  $5s\sigma(v=3)$  Rydbergs, as shown in Fig. 1. We were able to show that both transitions contribute and to confirm our spectral assignments by measuring the angular distribution of the products and comparing to the theoretical prediction.

The angular distribution expected following excitation of a selected rotational transition from case *a* coupling to case *b* coupling through an intermediate of case *b* is given by,

$$I(\theta) = \sum_M \left| D_{\Lambda', \epsilon' \leftarrow \Lambda'', \epsilon''}^{(2)}(J', N', J'', N'', M) \sum_{M_S} \left\{ \begin{array}{l} \langle N' \Lambda', SM_S | J' M \rangle d_{M \Lambda'}^{J'}(\theta) \\ \pm \langle N' - \Lambda', SM_S | J' M \rangle d_{M - \Lambda'}^{J'}(\theta) \end{array} \right\} \right|^2$$

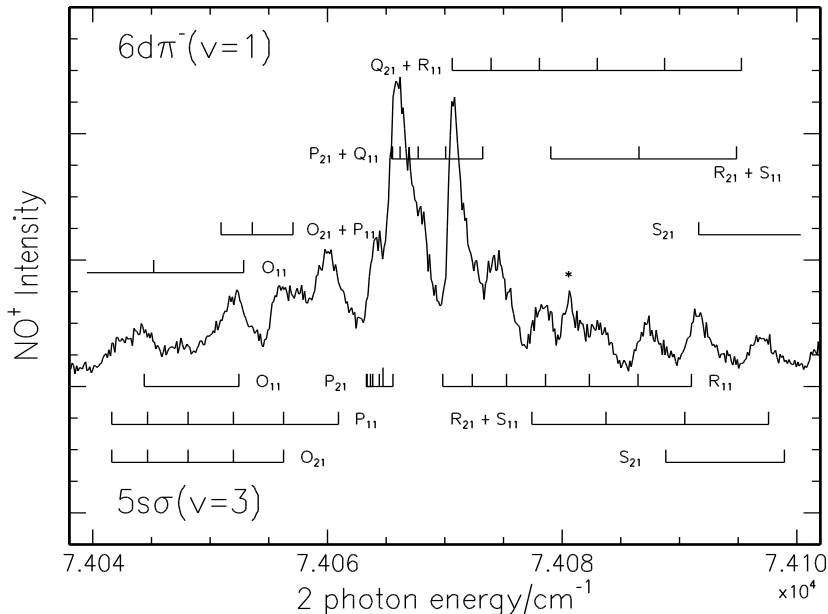


FIG. 1: Two-photon ionization spectra of NO as a function of the two-photon energy. Ionization of the  $6d\pi^-(v=1)/5s\sigma(v=3)$  bands using 100% NO. Top assignments correspond to  $6d\pi^-(v=1)$ , while bottom assignments belong to  $5s\sigma(v=3)$ .

where  $M$  is the projection of the rotational angular momentum onto the direction of the linear polarization of the excitation laser,  $D$  is a line-strength factor, and the two terms in the second summation are Clebsch-Gordan factors multiplied by rotation matrices; the  $+/-$  sign is used for positive/negative parity levels. The angular distribution is very sensitive to the rotational level and branch and to the symmetries of the intermediate electronic state in the two-photon excitation scheme, over which  $D$  is a summation.

Figure 2 shows the comparison between the calculated angular distributions based on the formula above and those measured following excitation to lines assigned to particular transitions. The good agreement between prediction and measurement gives confidence to our assignments. Not all assignments agreed so well, but all those that did not shared a particular intermediate and final level, thought to be perturbed. The angular distributions for this and for the other Rydberg levels studied could be fit only if it was assumed in the calculation that nearly all of the two-photon amplitude for the excitation went through an intermediate state of  $\Pi$  symmetry, probably the  $C^2\Pi$  state.

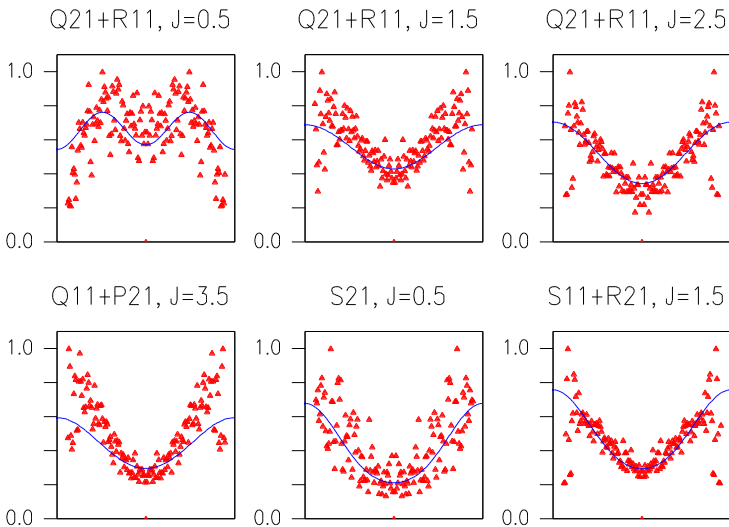


FIG. 2: Comparison between measured and predicted angular distributions. The  $x$  axis in all cases is from 0 to  $\pi$  radians.

## II. QUANTUM YIELDS FOR PRODUCT FORMATION IN THE 120–133 nm PHOTODISSOCIATION OF O<sub>2</sub>

Oxygen is a molecule of fundamental importance to atmospheric chemistry, but surprisingly little is known about its highly excited electronic states. We have studied the photodissociation of O<sub>2</sub> in the region from 120–133 nm by using product imaging. The spectrum in this region is dominated by transitions from the ground state  $u$  to the first three vibrational levels of the  $E^3\Sigma_u^-$  state. As shown in Fig. 3, the O(<sup>1</sup>D) + O(<sup>3</sup>P) channel is the only product channel observed by product imaging for dissociation at 124.4 nm; this is also true at 120.4 nm. The figure shows the velocity distributions of the O(<sup>1</sup>D) product (top) and the O(<sup>3</sup>P<sub>2</sub>) product (bottom) for dissociation at 124.4 nm. Peaks in both panels correspond to the production of the O(<sup>1</sup>D) + O(<sup>3</sup>P) channel, but there are no peaks corresponding to other possible channels. Similar data was obtained concerning the velocity distribution of the O(<sup>1</sup>D) product for dissociation at 120.4 nm. Again, a peak in the distribution corresponds to production of O(<sup>1</sup>D) + O(<sup>3</sup>P), but no peak is observed for the channel producing O(<sup>1</sup>D) + O(<sup>1</sup>D). We conclude that the quantum yield for O(<sup>1</sup>D) production at both wavelengths is unity.

The O(<sup>1</sup>D<sub>2</sub>) product is aligned in the molecular frame in such a way that its  $\mathbf{J}$  vector is perpendicular to the relative velocity vector between the O(<sup>1</sup>D) and the

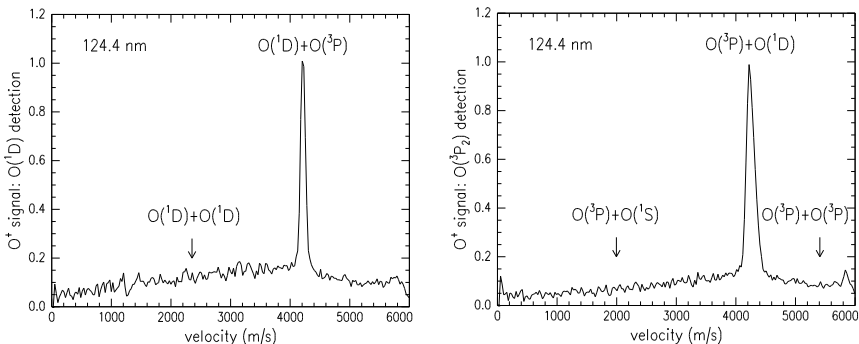


FIG. 3: Speed distributions of  $O(^1D)$  (left panel) and  $P(^3P)$  (right panel) produced in the 124.4 nm dissociation of  $O_2$ .

$O(^3P)$ . The repulsive part of the  $O_2(E^3\Sigma_u^-)$  state is actually the continuation of the repulsive part of the  $O_2(B^3\Sigma_u^-)$  state, which correlates to the observed  $O(^1D) + O(^3P)$  products, as shown in Fig. 4. According to the Wigner-Witmer rules, the combination of  $^1D$  and  $^3P$  atoms to produce a  $\Sigma$  state can only occur with  $m_J = 0$  or 1. This prediction is consistent with our finding that  $m_J = 0$  is strongly preferred.

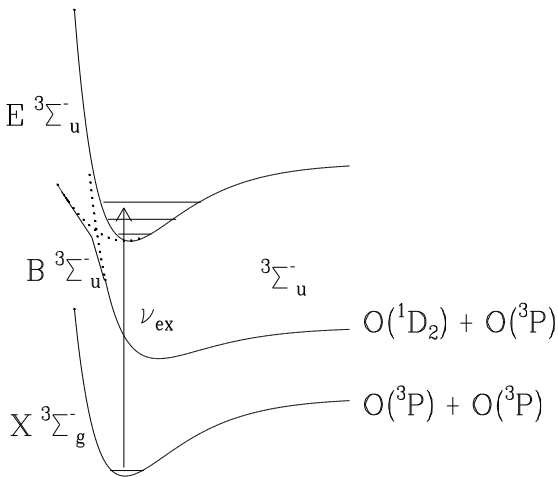


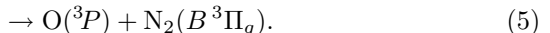
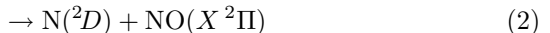
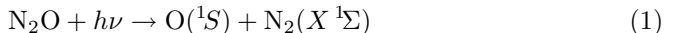
FIG. 4: Schematic diagram of  $O_2$   $X$ ,  $B$ , and  $E$  states.

At a dissociation wavelength of 132.7 nm, both the  $O(^1D) + O(^3P)$  and the  $O(^3P) + O(^3P)$  channels are observed with branching ratios of  $0.40 \pm 0.08$  and  $0.60 \pm 0.09$ , respectively. At 130.2 nm, the quantum yield for production of  $O(^1D)$  is  $0.76 \pm 0.28$ .

### III. PHOTODISSOCIATION OF $N_2O$ NEAR 130 nm

Nitrous oxide is an important component of Earth's natural atmosphere produced primarily by biological processes in soils and oceans. Mostly inert in the troposphere, it is transported to the stratosphere where it is destroyed both by photodissociation (at  $\lambda \approx 200$  nm),  $N_2O + h\nu \rightarrow N_2(X^1\Sigma) + O(^1D)$  and by reaction with  $O(^1D)$  produced either in the photodissociation or from the dissociation of ozone,  $N_2O + O(^1D) \rightarrow N_2 + O_2$  and  $\rightarrow NO + NO$ . NO produced in the second reaction is the primary catalytic agent destroying stratospheric ozone in the natural atmosphere.

At shorter wavelengths,  $N_2O$  can be excited to the  $C(^1\Pi)$  state near 145 nm or to the  $D(^1\Sigma^+)$  state near 130 nm. The absorption coefficient for the latter transition is high, about 80 Mb ( $1 \text{ Mb} = 10^{-18} \text{ cm}^2$ ). Although dissociation process (1) near 200 nm has been extensively studied, that at shorter wavelengths is both more complex and less well understood. At 130 nm, the following channels are thought to be important:



We have investigated channels (1)–(5) by using product imaging to detect the angular distributions for the five channels as well as the kinetic energy release for each of the product atoms or diatoms. The atomic products were probed by resonant ( $1+1'$ ) ionization using ultraviolet excitation for the first step, while the diatomic products were probed by non-resonant ionization. Our work is part of a larger effort at Cornell to characterize this photodissociation process. Witinski, Ortiz-Suárez, and Davis have used oxygen Rydberg time-of-flight spectroscopy to study channels (4) and (5), with results that are in reasonable agreement with ours [2].

Figure 5 shows the total kinetic energy release for the  $O + N_2$  products based on measurements of the  $O(^1S)$ ,  $O(^3P_0)$ ,  $O(^3P_2)$ , and  $N_2$  products. In each case, conservation of momentum is assumed to determine the total kinetic energy release. The good match for the  $N_2$  and  $O(^3P)$  peaks in the lower panel shows

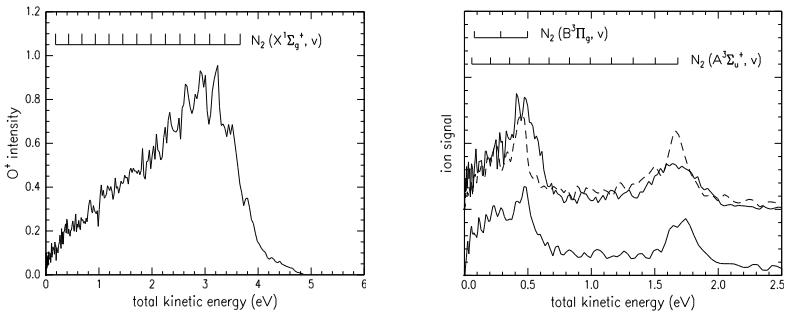


FIG. 5: Total kinetic energy released for O+N<sub>2</sub> products from the dissociation of N<sub>2</sub>O at 130.2 nm. Left: O(<sup>1</sup>S). Right: O(<sup>3</sup>P<sub>2</sub>) top solid curve; O(<sup>3</sup>P<sub>0</sub>) top dashed curve; N<sub>2</sub><sup>+</sup> bottom curve.

that these are indeed momentum matched. Similar data was obtained for the N+NO channel, where N(<sup>2</sup>D), N(<sup>2</sup>P), and NO were probed. In each of these cases, the energy release data provides information about the vibrational distribution of the diatomic fragment.

Information about the branching ratio between various channels has also been obtained. The ratio of O+ and NO+ can be converted to a branching ratio between the dissociation channels leading to O(<sup>3</sup>P)+N<sub>2</sub> vs. N+NO by calibrating against the O<sup>+</sup> and NO<sup>+</sup> peaks obtained from the dissociation of NO<sub>2</sub> at 355 nm, assuming that the vibrational distributions for NO in the NO<sub>2</sub> dissociation and the N+NO products are not too different. The reaction appears to favor the O(<sup>3</sup>P)+N<sub>2</sub> channel by a ratio of 1.4±0.5. Vacuum ultraviolet line strengths for O(<sup>3</sup>P) and O(<sup>1</sup>S) are known, so that correcting for laser power variations and assuming similar ionization efficiencies, we find that the O(<sup>1</sup>S)+N<sub>2</sub>(X) channel has about 10±1.5 times the quantum yield of the O(<sup>3</sup>P)+N<sub>2</sub>(A,B) channel. Spin-orbit distributions have also been obtained for all atomic products, and the ratio of quantum yields for the N(<sup>2</sup>D)+NO vs. N(<sup>2</sup>P)+NO channels is about 3.

- 
- [1] S. T. Pratt, Ch. Jungen and E. Miescher, J. Chem. Phys. **90**, 5971 (1989).  
 [2] M. F. Witinski, M. Ortiz-Surez and H. F. Davis, J. Chem. Phys. **122**, 174303 (2005).